Water-Soluble α,β-Unsaturated Aldehydes of Cigarette Smoke Induce Carbonylation of Human Serum Albumin

Graziano Colombo,[1] Giancarlo Aldini,[2] Marica Orioli,[2] Daniela Giustarini,[3] Rosalba Gornati,[4] Ranieri Rossi,[3] Roberto Colombo,[1] Marina Carini,[2] Aldo Milzani,[1] and Isabella Dalle-Donne[1]

Abstract

Cigarette smoking is a major risk factor for developing pulmonary and cardiovascular diseases as well as some forms of cancer. Understanding the mechanisms by which smoking contributes to disease remains a major research focus. Increased levels of carbonylated serum proteins are present in smokers; albumin is the major carbonylated protein in the bronchoalveolar lavage fluid of older smokers. We have investigated the susceptibility of human serum albumin (HSA) to α,β-unsaturated aldehyde-induced carbonylation when exposed to whole-phase cigarette smoke extract (CSE). Fluorescence studies with fluorescent probes showed depletion of HSA Cys34 free thiol and marked decrease of free Lys residues. Spectrophotometric and immunochemical carbonyl assays after carbonyl derivatization with 2,4-dinitrophenylhydrazine revealed the formation of covalent carbonyl adducts. Nanoscale capillary liquid chromatography and electrospray tandem mass spectrometry analysis detected acrolein and crotonaldehyde Michael adducts at Cys34, Lys525, Lys351, and His39 at all the CSE concentrations tested. Lys541 and Lys545 were also found to form a Schiff base with acrolein. The carbonyl scavenger drugs, hydralazine and pyridoxamine, partially prevented CSE-induced HSA carbonylation. Carbonylation of HSA associated with cigarette smoking might result in modifications of its antioxidant properties and transport functions of both endogenous and exogenous compounds. *Antioxid. Redox Signal.* 12, 349–364.

Introduction

CIGARETTE SMOKING is one of the major risk factors for developing pulmonary and cardiovascular diseases like emphysema, chronic bronchitis, chronic obstructive pulmonary disease, myocardial infarction, and atherosclerosis, as well as some forms of malignancies, particularly lung and throat cancer (9).

Whole cigarette smoke (CS) is a complex aerosol consisting of a vapor and particulate phase, containing at least 4,800 identified constituents (28), although most of these are present in vanishingly small concentrations. Many noxious compounds in cigarette smoke act as oxidants, proinflammatory agents, carcinogens (or a combination of these), or tumor promoters (28, 46). In addition to nicotine, identified compounds include pyridine alkaloids, ammonia, phenols, *N*-nitrosamine, polycyclic aromatic hydrocarbons, quinones, benzo(*a*)pyrene, hydrogen cyanide, carbon monoxide and

dioxide, and reactive oxygen/nitrogen species (ROS/RNS) (28, 33). In addition, cigarette smoke contains high concentrations of reactive volatile aldehydes, such as acetaldehyde, formaldehyde (saturated aldehydes) and α,β-unsaturated aldehydes, including acrolein (2,3-propenal) and crotonaldehyde (2-butenal), which are particularly harmful because of their high reactivity and high toxicity.

α,β-Unsaturated aldehydes, though reactive, are long-lived compared with most ROS/RNS and oxidizing intermediates, possessing half-lives ranging from a few hours to days, and then can diffuse long distances before reacting with proteins, so acting as "toxic second messengers" (1). Acrolein and other aldehydes are present in saliva or exhaled breath condensate in low micromolar concentrations in healthy subjects and are elevated up to 10-fold in heavy smokers (5, 6). Exposure of saliva to crotonaldehyde and acrolein, at concentrations known to be present in CS, resulted in an increase of protein carbonyls and a parallel decrease in -SH groups (53).

[1]Dipartimento di Biologia, and [2]Dipartimento di Scienze Farmaceutiche "Pietro Pratesi," Università degli Studi di Milano, Milan, Italy.
[3]Department of Evolutionary Biology, University of Siena, Siena, Italy.
[4]Department of Biotechnology and Molecular Sciences, University of Insubria, Varese, Italy.

Exposure of human plasma to gas-phase CS produces protein carbonyl accumulation and loss of protein sulfhydryl groups (47), aldehydes contained in CS being chiefly responsible for the observed protein modifications (41). Exposure to CS (or inhaled acrolein) results in the formation of specific protein–acrolein adducts in the lung, plasma, and in the aorta of exposed mice (15). These observations suggest that, despite its high reactivity, free acrolein is transported from the lung into systemic circulation and to vascular sites (15). Smokers' urine contains high concentrations (6–8 μM) of acrolein metabolites, demonstrating the presence of systemic acrolein and the contribution of acrolein metabolism (13).

The common feature of α,β-unsaturated aldehydes (reactive carbonyl species) is the presence of an unsaturated carbonyl group that confers on them the capacity to form stable covalent adducts with nucleophilic amino acids (*i.e.*, Cys, His, and Lys residues in proteins), often resulting in protein carbonylation (2, 3, 17, 18). Introduction of carbonyl groups into amino acid residues is the most general byproduct of protein oxidative damage and quantification of carbonyl content, determined as 2,4-dinitrophenylhydrazine (DNPH) derivatives, is generally used to estimate the oxidative damage of proteins (20, 30, 31).

Increased levels of protein carbonyls have been found in serum proteins of smokers compared with nonsmokers (34, 45), whereas no difference was seen between heavy and light smokers (45). Furthermore, recent studies showed that albumin is the major carbonylated protein in the bronchoalveolar lavage fluid of older smokers with long-term smoking histories, even in the absence of lung diseases (36, 50).

Several approaches have been used to evaluate CS. Typically, cells and protein solutions are exposed to smoke extracts. Because of the ease of collection, the most common methods of collecting CS include bubbling whole CS through an aqueous solution, usually phosphate-buffered saline (PBS), to collect the aqueous phase of gas/vapor phase (cigarette smoke extract, CSE), or sampling total particulate matter (TPM) on a Cambridge filter (a standard glass-fiber Cambridge filter pad that retains 99.9% of all particulate matter with a size >0.1 μm), or by other trapping methods (thus collecting the particulate phase). CSE contains most of the components inhaled by smokers. The generation of CSE in aqueous solutions results in the collection of only the water-soluble components of whole CS (14). CSE is added to the culture medium of a cell culture or to protein solutions, at different dilutions. TPM is extracted with an organic solvent, usually dimethyl sulfoxide, to collect the lipid-soluble phase (cigarette smoke condensate, CSC), and the organic extract is then added to the cell-culture medium or to protein solution. To study the effects of native CS in cell culture, direct-exposure methods have been developed. Whole-phase CS solution can be prepared with a homemade "apparatus" (consisting of a glass Erhlenmeyer flask with a side arm, a 500-μl pipette tip, and a water pump) so devised as to simulate the manner in which the respiratory tract lining fluid is exposed to CS during the process of smoking by humans (43). The smoke is permitted to come into contact with the thin layer of buffer solution in the bottom of the flask, avoiding direct bubbling. The resultant dark yellow solution is termed whole-phase CS solution. The pH of the whole-phase CS solution is adjusted to 7.4 by addition of sodium hydroxide solution, after which it is filtered through a 0.22-μm Millipore filter.

Aqueous extract of CS can also be prepared by extracting thrice the whole-phase CS solution with an equal volume of diethyl ether. The aqueous extract is made free of solvent by applying a gentle suction under vacuum. This solution is termed aqueous extract of CS (43).

With extracts of smoke, the individual constituents of the crude smoke condensate mixture will be effective to a different extent, according to their physicochemical properties, mainly their solubility. The generation of CSE in aqueous solutions results in the collection of only the water-soluble (particulate) components of whole CS (14). Water-soluble components of CS can readily reach both the systemic circulation (16) and interstitial cells (29), suggesting that compounds found in CSE may mimic *in vivo* situations. This is further supported by observations that *in vivo* smoke exposure can mimic *in vitro* CSE challenge (16).

We describe here the susceptibility of human serum albumin (HSA) to α,β-unsaturated aldehyde-induced carbonylation when exposed to whole-phase CSE, which is widely used as a model system to study *in vitro* effects of CS (14, 16, 43).

Materials and Methods

Chemicals

Delipidized crystalline HSA (∼ 99% agarose gel electrophoresis), DNPH, fluorescamine (4-phenyl-spiro [furan-2(3H), 1'-phthalan]-3,3'-dione), hydralazine, pyridoxamine dihydrochloride, and LC-MS grade solvents (Chromasolv) were purchased from Sigma-Aldrich Chemie GmbH (Milan, Italy). *N*-[6,7-(amino-4-methylcoumarin-3-acetamido)hexyl]-3'-[2'-pyridyldithio] propionamide (AMCA-HPDP) was obtained from Pierce Biotechnology (Rockford, IL). Anti-dinitrophenyl-KLH antibodies, rabbit IgG fraction and goat anti-rabbit IgG, horseradish peroxidase conjugate were purchased from Molecular Probes (Eugene, OR). ECL Plus Western blotting detection reagents were purchased from Amersham Biosciences Europe GmbH (Milan, Italy). Sequence grade-modified trypsin was obtained from Promega (Milan, Italy). All other reagents were of analytic grade. Research-grade cigarettes (3R4F) were purchased from the College of Agriculture, Kentucky Tobacco Research & Development Center, University of Kentucky (USA).

Preparation of whole-phase cigarette smoke extract

Whole-phase CSE from Kentucky 3RF4 reference cigarettes was prepared as previously described (43). Mainstream smoke from one cigarette (10 puffs) was allowed to dissolve (for 10 s each puff) in 1 ml of 50 mM potassium phosphate buffer (PBS), pH 7.4. The resultant dark yellow solution was defined as 100% whole-phase CSE and was filtered through a 0.22-μm Millipore filter (Bedford, MA) to remove bacteria and large particles. The pH of the whole-phase CSE was adjusted to 7.4 by addition of 2 M sodium hydroxide solution. To ensure standardization between experiments and batches of CSE, CSE preparations were made uniform by measurement of absorbance at 340 nm. CSE was freshly prepared immediately before use for each experiment and diluted to an appropriate concentration with 50 mM PBS.

Preparation of human mercaptalbumin (HSA-SH)

Delipidized serum albumin (12 mg/ml, 0.18 mM) was quantitatively converted to mercaptalbumin (HSA-SH), in

which the single thiol of HSA is completely reduced, by treatment with 1.5 mM DTT in 50 mM PBS, pH 7.4, for 15 min at room temperature. The excess of DTT was then removed by exhaustive dialysis against 50 mM PBS, pH 7.4.

Exposure of HSA-SH to CSE

HSA-SH (molecular mass, 66.486 kDa) concentration was determined by measuring the absorbance at 280 nm, by using an extinction coefficient of 39,800 M/cm. HSA-SH (4 mg/ml, 60 μM) was treated for 60 min, at 25°C, with various concentrations of CSE (1%, 4%, 16%, and 64%, vol/vol), with gentle rotary shaking. The removal of CSE was accomplished with exhaustive dialysis against PBS at 4°C. As the whole-phase CSE reveals an intrinsic fluorescence when measured by using an excitation wavelength of 340 nm and an emission wavelength of 440 nm, at 25°C, complete CSE removal was checked by measuring its related fluorescence in the dialysis buffer. All reported experiments were carried on in CSE-free buffer.

Labeling of HSA free sulfhydryl group with AMCA-HPDP

After treatment with various concentrations of CSE, HSA samples (400 μg) were mixed with three volumes of 100% acetone, and protein was allowed to precipitate for 30 min at −20°C, followed by centrifugation at 10,000 g for 10 min, at 4°C. Protein pellets were resuspendend in AMCA-HPDP solution (100 μM in 50 mM phosphate buffer, pH 7.4) at a molar ratio of 1:6 in favor of AMCA-HPDP. Samples were incubated for 60 min at room temperature in the dark to ensure complete blocking of exposed sulfhydryl groups. AMCA-HPDP-labeled HSA samples were precipitated with acetone, as in the previous step, and resuspended with an equal volume of 2× nonreducing Laemmli SDS-PAGE sample buffer.

Detection of HSA sulfhydryl group with AMCA-HPDP by SDS-PAGE

Approximately 10 μg protein for each sample was loaded on 10% SDS-PAGE. At the end of the electrophoretic run under nonreducing condition, the gel was rinsed with Milli-Q water and transferred to the platform surface of a UV transilluminator ($\lambda_{exc} = 340$ nm). On UV activation, brilliant blue bands of HSA could be seen by the naked eye and were recorded by a camera, Canon S5IS. Densitometric analysis was performed after scanning the gels by using Image J 1.40d (National Institutes of Health, Bethesda, MD).

Albumin-AMCA-HPDP fluorescence-emission spectrum

The fluorescence-emission spectrum of AMCA-HPDP-labeled HSA (0.2 μM) was determined at 25°C by using an excitation wavelength of 345 nm and scanning at emission wavelengths from 360 to 550 nm. Fluorescence data were collected with a Kontron SFM-25 spectrofluorometer, by using 10×10 mm quartz cuvettes.

Quantification of lysine residues

Lysine residues were measured with fluorescamine fluorescence (19). The nonfluorescent compound fluorescamine reacts with primary amino groups in a matter of milliseconds to produce a fluorescent product, whereas unreacted fluorescamine hydrolyzes in a matter of seconds to nonfluorescent products, effectively removing it from the reaction. In a typical assay, 270 μl of control or CSE-treated HSA (2.66 μM) was added to 1.35 ml of sodium borate buffer (200 mM, pH 8.5) and mixed; 180 μl of fluorescamine (1 mM in acetone) was added with vortexing. After incubation at 25°C for 15 min in the dark, fluorescence was measured between 400 and 600 nm by using an excitation wavelength of 390 nm. All albumin samples were diluted appropriately in borate buffer to yield a range of fluorescence in which a linear relation between fluorescence and amine concentrations was observed. The fluorescence of CSE-treated albumin was expressed relative to that of HSA-SH (control sample), considered as 100%.
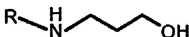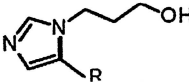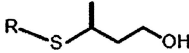
Quantification of arginine residues
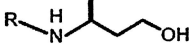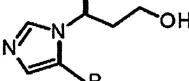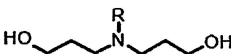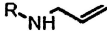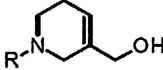
The amount of free arginine residues in CSE-treated HSA was determined by using 9,10-phenanthrenequinone reagent (49). In this assay, 200-μl HSA samples (0.5 mg/ml, 7.5 μM, in 50 mM PBS, pH 7.4) were mixed with 600 μl of 9,10-phenanthrenequinone (150 μM in ethanol) and 100 μl NaOH (2 M) and incubated at 60°C for 3 h. After incubation, 900 μl HCl (1.2 M) was added to each sample and incubated in th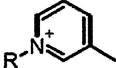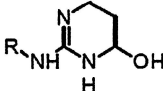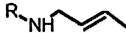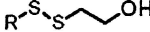e dark at room temperature for 1 h. The fluorescence-emission spectrum of labeled HSA (0.8 μM) was determined at 25°C by using an excitation wavelength of 312 nm and scanning at emission wavelengths from 300 to 600 nm. Fluorescence data were collected with a Kontron SFM-25 spectrofluorometer, by using 10×10 mm quartz cuvettes.

NanoLC-MS/MS analysis

The CSE-induced structure modifications of HSA were characterized with nanoscale capillary liquid chromatography and electrospray tandem mass spectrometry (nanoLC-ESI-MS/MS) analysis of incubated samples after reduction with NaBH$_4$, an established procedure for adduct stabilization, followed by enzymatic digestion with trypsin. Peptide mass mapping provided identification of the peptides, accounting for ∼80–90% of the protein sequence, as previously reported (3).

All digested peptide mixtures were separated with online reversed-phase (RP) nanoscale capillary liquid chromatography (nanoLC) and analyzed with electrospray tandem mass spectrometry (ESI-MS/MS). Chromatography was performed by using a Surveyor LC system (ThermoFinnigan Italia, Milan, Italy) on a 180 μm×10 cm column packed with 5-μm Biobasic-18 stationary phase (Thermo, Superchrom, Milan, Italy). The pump flow rate was split 1:75 for a column flow rate of 1 μl/min. The column effluent was directly electrosprayed by using the silica emitter source without further splitting. Mobile phases A and B were 0.1% formic acid in water and in methanol, respectively. The separation of peptides obtained with enzymatic digestion was achieved with a gradient of 0–100% B over a 65-min period. Before the next analysis, both the precolumn and the column were first washed with 100% solvent B for 10 min and then equilibrated with 100% solvent A for 20 min. For the identification of peptides, an LTQ XL-Orbitrap mass spectrometer was used (Thermo Scientific, Milan, Italy), and the electrospray interface (dynamic nanospray probe; Thermo Scientific, Milan, Italy) was set as follows: spray voltage, 1.6 Kv; capillary

TABLE 1. PREDICTED ACROLEIN AND CROTONALDEHYDE COVALENT ADDUCTS ON CYS, HIS, AND LYS RESIDUES

Modification	Target amino acid	Structure	Mass shift (Da, isotopic value)
ACR Michael adduct (reduced form)	Cys		58.04186
	Lys		58.04186
	His		58.04186
CRO Michael adduct (reduced form)	Cys		72.05751
	Lys		72.05751
	His		72.05751
ACR double Michael adduct (reduced form)	Lys		116.15828
ACR Schiff base (reduced form)	Lys		40.0313
FDP-lysine (reduced form)	Lys		96.05751
MP-lysine (reduced form)	Lys		77.03912
Arginine adduction by ACR	Arg		56.02621
CRO Schiff base (reduced form)	Lys		54.09044
Mercaptoethanol disulfide	Cys		75.99829

ACR, acrolein; CRO, crotonaldehyde; FDP-lysine, N(epsilon)-(3-formyl-3,4-dehydropiperidino)lysine; MP-lysine, N(epsilon)-(3-methylpyridinium)lysine.

FIG. 1. **Three-dimensional structure of human serum albumin (HSA) and location of Cys, His, and Lys residues.** HSA atomic coordinates were downloaded from the Protein Data Bank, accession code 1AO6 (20), and the figure was generated by using the Swiss-PdbViewer (25). In HSA primary structure (*lower panel*), individual amino acid residues are indicated with the single-letter code. Positions of Cys, His, and Lys residues are shown and colored in accordance with their relative accessibility to the solvent, defined as described in Materials and Methods. (For interpretation of the references to color in this figure legend, the reader is referred to the web version of this article at www.liebertonline.com/ars).
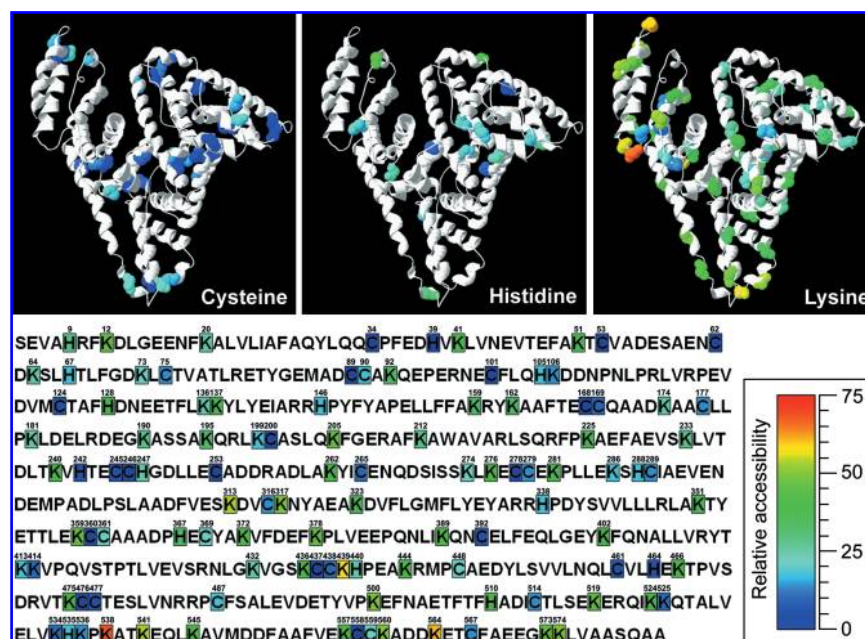
temperature, 220°C; capillary voltage, 30 V; tube lens offset, 120 V; no sheath or auxiliary gas flow. The analyses were performed in positive polarity enabling the data-dependent scan mode. The MS spectra were acquired in profile mode by Orbitrap in the following conditions: scan range, 250–2,000 m/z in full-scan mode with full-scan injection waveforms enabled; the AGC target setting was 5×10^5; maximum inject time, 500 ms; scan time, 1 s (60,000 res. Pwr. at 400 m/z, FWHM). A list of 14 protonated phthlates and siloxanes including dibutylphthlate (plasticizer, m/z 279.159086), bis (2-ethylhexyl)phthalate (m/z 391.284286) and dodecamethylcyclohexasiloxane [$(Si(CH_3)_2O)_6 + H]^+$; m/z 445.120025] was used for real-time internal mass calibration (40). Tandem mass spectra were recorded by the linear ion trap in centroid mode for the three most-intense ions (isolation width, 2 m/z; normalized collision energy, 35 CID arbitrary units; minimum signal threshold, 5×10^4), and dynamic exclusion was enabled (repeat count, three; repeat duration, 10 s; exclusion list size, 25; exclusion duration, 120 s; relative exclusion mass width, 5 ppm). Charge-state screening and monoisotopic precursor selection was enabled; singly and unassigned charged ions were rejected.

Acrolein and crotonaldehyde adduct identification

The acquired MS/MS spectra were searched by using the Bioworks software (rev. 3.3.1 sp1; Thermo Scientific, Milan, Italy) and by using a database containing only the protein of interest. The following settings were used for the search engine: mass type, monoisotopic precursor and fragments; enzyme, trypsin (KR); missed cleavage sites, five; peptide tolerance, 5 ppm; fragmentations tolerance, 0.5 AMU; modifications, 5 PTMs per peptide; the variable modifications considered are listed in Table 1. Results were filtered by setting the peptide probability to 0.005. Peptide ion responses were determined by measuring the peak areas in the selected ion chromatograms (SICs) reconstituted by using the most abundant multicharged filter ions. The peptide responses were normalized in respect to peptide LSQR ([M + H]$^+$ at m/z

503.2955), chosen as reference peptide because it does not contain nucleophilic residues.

Spectrophotometric assay with DNPH

Carbonyl groups formed on HSA were quantified by adding an equal volume of 10 m*M* DNPH in 2 *M* HCl to solutions containing the control or CSE-treated protein (400 μg). Samples were allowed to stand in the dark at room temperature for 1 h, with vortexing every 10 min. Samples were precipitated with trichloroacetic acid (TCA; 20% final concentration, 15 min on ice) and centrifuged at 10,000 *g* in a tabletop microcentrifuge for 5 min, at 4°C. The supernatants were discarded, and the protein pellets were washed once more with TCA and then washed 3 times with 1-ml portions of ethanol/ethylacetate (1:1) to remove any free DNPH. The protein samples were resuspended in 1 ml of 6 *M* guanidine hydrochloride (dissolved in 50 m*M* phosphate buffer, pH 2.3) at 37°C for 15 min with vortex mixing. Carbonyl contents were determined from the absorbance at 366 nm by using a molar absorption coefficient of 22,000 M/cm (32).

Western blot analysis with anti-DNP antibody

Carbonyl groups formed on HSA were determined with Western immunoblotting (18). After SDS-PAGE separation on 10% (wt/vol) polyacrylamide gels of ~10 μg protein for each sample, samples were blotted to an immobilon P membrane followed by successive incubations in 2 *M* HCl and DNPH (0.1 mg/ml in 2 *M* HCl) for 5 min each. The membrane was then washed 3 times in 2 *M* HCl and 7 times in 100% methanol for 5 min each, followed by one wash in PBST [10 m*M* Na-phosphate, pH 7.2, 0.9% (wt/vol) NaCl, 0.1% (vol/vol) Tween 20] and blocking for 1 h in 5% (wt/vol) nonfat dry milk in PBST. After washing 3 times with PBST for 5 min each, carbonyl formation was probed by 2-h incubation with 5% milk/PBST containing anti-dinitrophenyl-KLH (anti-DNP) antibodies (1:10,000 dilution). After three washes with PBST for 5 min each, the membrane was incubated with a 1:2,000
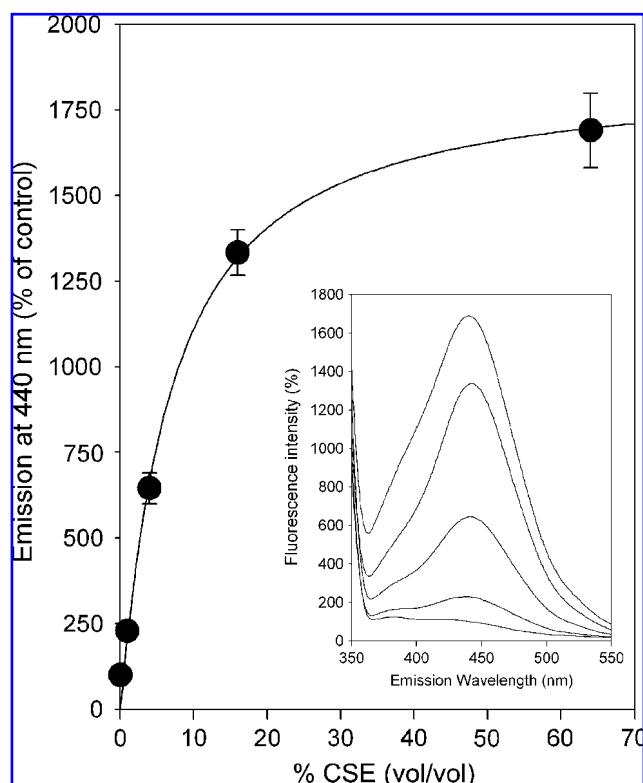
FIG. 2. Whole-phase CSE-induced fluorescence emission intensity of HSA. HSA-SH was exposed to 1%, 4%, 16%, and 64% (vol/vol) CSE and exhaustively (48 h) dialyzed against PBS, with several changes. All experiments were carried on in CSE-free media. HSA samples exposed to increasing concentrations of CSE show an increase in the 350- to 550-nm fluorescence emission intensity after excitation at 340 nm, with an intensity peak at 440 nm, indicating that some components of CSE, which shows autofluorescence when analyzed under the same emission and excitation wavelengths, were bound to HSA. Maximum fluorescence-emission intensity at 440-nm wavelength *vs.* CSE concentration is shown. The maximum value of fluorescence emission intensity of control HSA (HSA-SH) was considered as 100%. Data are presented as the mean ± SD of three replicate measurements. (*Inset*) Fluorescence-emission spectra at excitation wavelength of 340 nm. From top to bottom: HSA treated with 64%, 16%, 4%, and 1% CSE or vehicle (control).

dilution of the secondary antibody linked to horseradish peroxidase in 5% milk/PBST for 1 h. After washing 3 times with PBST for 5 min each, immunostained protein bands were visualized with enhanced chemiluminescence detection. Densitometric analysis was performed after scanning the chemiluminescence films by using Image J 1.40d (National Institutes of Health).

Carbonylation scavenging assays

The activity of various carbonyl scavengers toward CSE-induced HSA carbonylation was investigated by incubating HSA-SH (4 mg/ml, 60 μM) for 60 min, at 25°C, with various concentrations (10 and 100 μM, 1 mM) of hydralazine and pyridoxamine, with gentle rotary shaking, before exposing the different protein solutions to 1%, 4%, 16%, or 64% (vol/vol) CSE, for 60 min, at 25°C, with gentle rotary shak-

ing. The removal of carbonyl scavengers and CSE was accomplished by protein precipitation with 20% (final concentration) TCA, for 15 min on ice, and centrifugation at 10,000 *g* in a tabletop microcentrifuge for 5 min, at 4°C. The supernatants were discarded, and the protein pellets were washed once more with 20% TCA; the protein pellets were then resuspended in PBS to 1 mg/ml ($\sim$15 μM) HSA (final concentration) before quantifying protein carbonylation by the spectrophotometric assay with DNPH, as described earlier.

Molecular modeling and amino acid residue relative accessibility

Molecular modeling and analysis of the relative accessibility of Cys, Lys, and His residues in the HSA molecule were performed by using the molecular visualization program Swiss-PdbViewer, version 4.0 (25). The figure was created on the basis of atom coordinates of HSA (PDB code 1AO6) (21). Maximum accessibility is defined as being the accessible surface of a Cys, Lys, and His residue in a pentapeptide GGaaGG in extended conformation. This scale differentiates core Cys, Lys, and His residues from surface ones. Dark blue color is attributed to completely buried amino acid residues, whereas red color is attributed to Cys, Lys, and His residues with at least 75% of their relative surface accessible.

Results

Albumin is a 66.5-kDa single-chain protein containing 585 amino acids (Fig. 1), 17 disulfide bonds (cystines), and only one free cysteine, Cys34 (Fig. 1A), which is completely conserved within mammalian albumins and provides the largest fraction ($\sim$80%) of free thiols in human plasma. It also contains 59 lysines (Fig. 1C) and nine histidines (Fig. 1B). Because Cys34 thiol is a notable scavenger of plasma reactive species/oxidants, mainly owing to its very high concentration ($\sim$0.4–0.5 mM) rather than to its fast reactivity with oxidants (52), the plasma albumin pool serves as a key element of intravascular/extracellular antioxidant defenses (12, 23, 30). Recently, we suggested that HSA, through nucleophilic residues, can act as an endogenous detoxifying agent of circulating reactive carbonyl compounds (4). Like other α,β-unsaturated aldehydes, acrolein and crotonaldehyde selectively react with the sulfhydryl group of cysteine, the imidazole group of histidine, and the ε-amino group of lysine (4, 18, 22). As the α, β-unsaturated aldehydes acrolein and crotonaldehyde are abundantly present in CS (53), they might react with HSA, leading to the formation of carbonylated albumin. The possible covalent modifications of the nucleophilic amino acids His, Lys, and Cys with acrolein and crotonaldehyde were predicted and, for each adduct, the isotopic mass shift of the corresponding reduced form was calculated (Table 1) and used as variable modification in the Sequest search.

Mercaptalbumin was treated for 60 min with various concentrations of whole-phase CSE (1%, 4%, 16%, and 64%, vol/vol), followed by exhaustive dialysis (48 h) against PBS, with several changes to assure complete CSE removal. HSA samples exposed to increasing concentrations of CSE show an increase in the 350–550 nm fluorescence-emission intensity after excitation at 340 nm, with a fluorescence maximum at 440 nm, indicating that some components of CSE, which shows autofluorescence when analyzed under the same

FIG. 3. Quantification of Cys34 thiol modification by using the sulfhydryl-specific fluorescent reagent AMCA-HPDP. HSA-SH solutions were treated with vehicle (control) or 1%, 4%, 16%, and 64% (vol/vol) CSE, exhaustively dialyzed against PBS, and labeled at Cys34-free -SH with AMCA-HPDP, as described in Materials and Methods. Conditions for protein separation by nonreducing SDS-PAGE, visualization of bound AMCA-HPDP, and subsequent gel staining with CBB were as described in Materials and Methods. (**A**) AMCA-HPDP–labeled HSA samples were analyzed with UV light exposure ($\lambda_{exc} = 340$ nm). (**B**) The same gel stained with CBB. (**C**) Densitometric analysis of AMCA-HPDP binding. Changes in fluorescence intensities of AMCA-HPDP-HSA bands in comparison with fluorescence of control HSA (HSA-SH), considered as 100%, are shown. Data are presented as the mean $\pm$ SD of three replicate measurements.
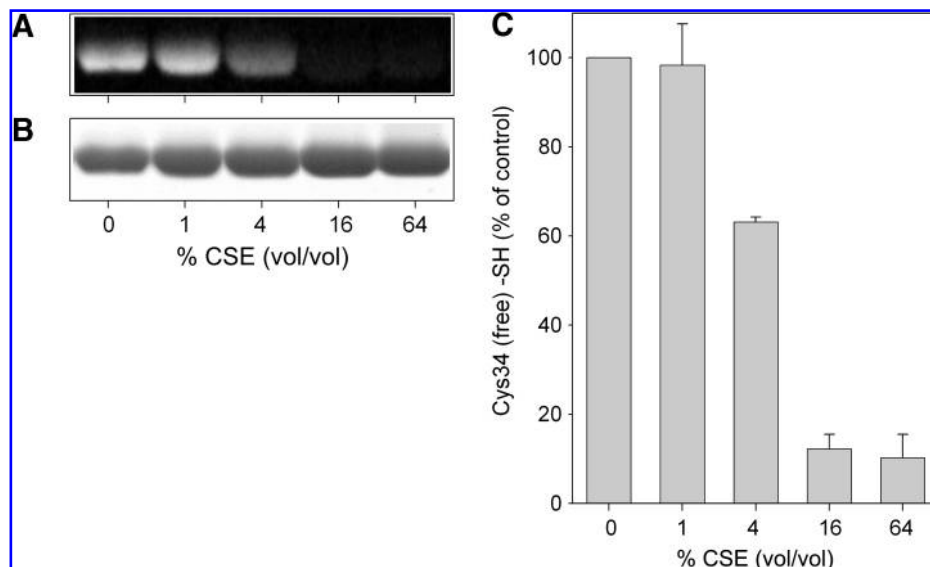

FIG. 4. Fluorescence-emission intensity of AMCA-HPDP–labeled HSA. HSA-SH solutions were treated with vehicle (control) or 1%, 4%, 16%, and 64% (vol/vol) CSE, exhaustively dialyzed against PBS, and labeled at Cys34-free -SH by AMCA-HPDP, as described in Materials and Methods. Maximum fluorescence-emission intensity at 432-nm wavelength *vs.* CSE concentration is shown. The maximum value of fluorescence-emission intensity of control HSA (HSA-SH) was considered as 100%. Data are presented as the mean $\pm$ SD of three replicate measurements. (*Inset*) Fluorescence-emission spectra at 345-nm excitation wavelength. From top to bottom: HSA treated with vehicle (control) or 1%, 4%, 16%, and 64% CSE.

FIG. 5. CSE-mediated blocking of Lys residues in CSE-treated HSA. HSA-SH solutions were treated with vehicle (control) or 1%, 4%, 16%, and 64% (vol/vol) CSE and exhaustively dialyzed against PBS. Quantification of modified (carbonylated) Lys residues was assessed by the decrease in fluorescamine fluorescence at excitation wavelength of 390 nm, as described in Materials and Methods. Maximum fluorescence-emission intensity at 463 nm *vs.* CSE concentration is shown. The maximum value of fluorescence-emission intensity of control HSA (HSA-SH) was considered as 100%. Data are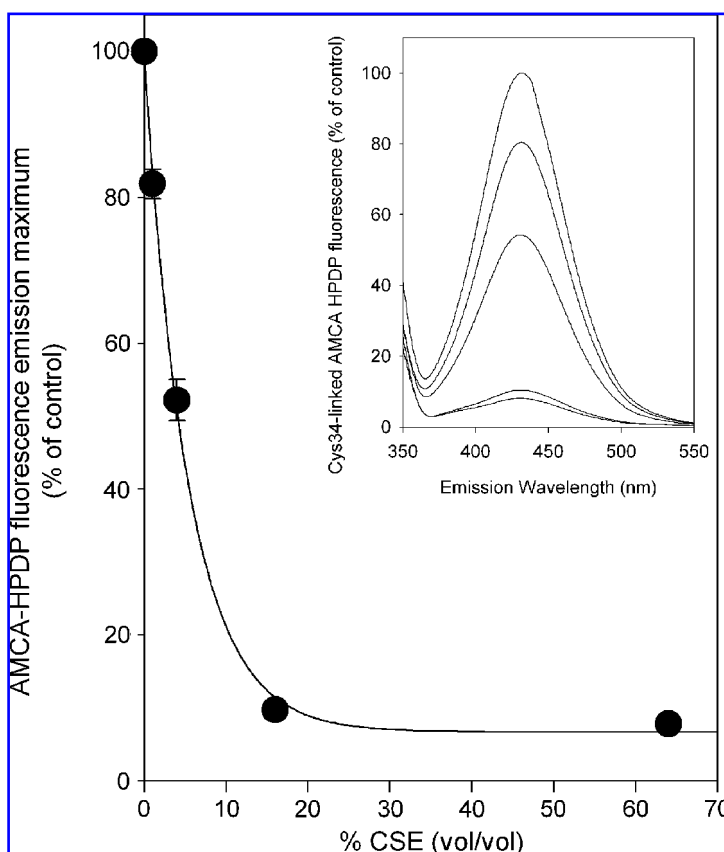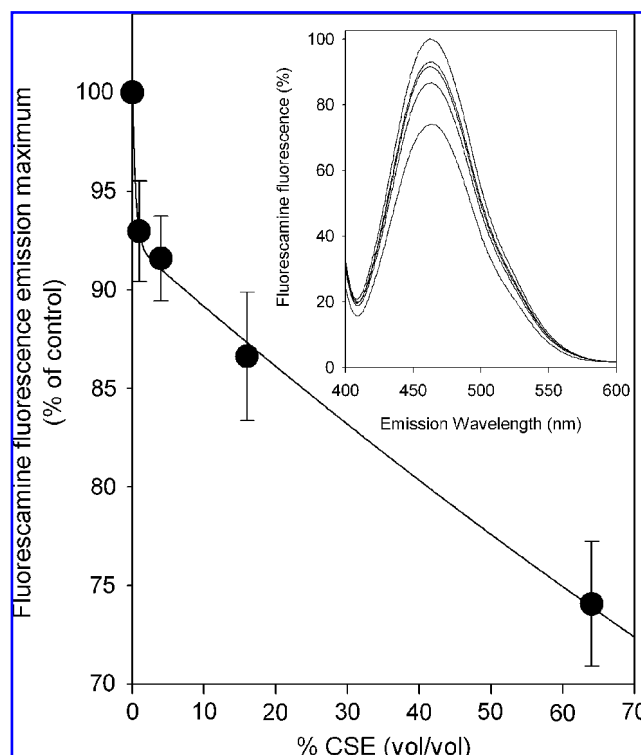 presented as the mean ± SD of three replicate measurements. (*Inset*) Fluorescence-emission spectra at 390 nm excitation wavelength. From top to bottom: HSA treated with vehicle (control) or 1%, 4%, 16%, and 64% CSE.

emission and excitation wavelengths, were bound to HSA (Fig. 2).

The identification of Cys34 as a target of CSE-induced protein modification was established by using AMCA-HPDP, a fluorescent probe that is specific for sulfhydryl groups (26). After separation by nonreducing SDS-PAGE, AMCA-HPDP–labeled albumin samples can be detected in gel on UV activation. In this case, the loss of the AMCA-HPDP signal is proportional to the degree of Cys34 thiol modification. The results of HSA labeling with AMCA-HPDP are presented in Fig. 3. HSA exposed to CSE clearly exhibited a decrease in the Cys34 sulfhydryl group relative to control HSA-SH (mercaptalbumin) (Fig. 3A). Comparison of the fluorescent image (Fig. 3A) with the CBB staining image (Fig. 3B) of the same gel demonstrated equal protein loading in each lane. Densitometric analysis of AMCA-HPDP binding to Cys34 thiol confirmed that the extent of labeling was drastically reduced in HSA exposed to 4% CSE and negligible in HSA exposed to more-concentrated CSE solutions (Fig. 3C).

The identification of Cys34 as a target of CSE-induced protein modification was further established in a complementary experiment by monitoring the AMCA-HPDP fluorescence-emission spectrum (Fig. 4, inset). When conjugated with CSE-treated HSA, AMCA-HPDP revealed a remarkable reduction in its fluorescence-emission spectrum, recorded between 350 and 550 nm (Fig. 4, inset). Modification of Cys34 thiol, evaluated by the loss of AMCA-HPDP binding and evidenced by the marked reduction of the fluorophore fluorescence-emission maximum, was quantified as 20% and 45% in HSA exposed to, respectively, 1% and 4% CSE (Fig. 4). Exposure of HSA to 16% and 64% CSE decreased the AMCA fluorescence to ∼10% of that of control HSA-SH (mercaptalbumin), considered as 100% (Fig. 4).

Together with cysteine, lysine residues are major targets for formation of carbonyl derivatives (20). The nonfluorescent compound, fluorescamine, reacts rapidly with primary amines in proteins, such as the terminal amino group of peptides and the ε-amino group of lysine, to form highly fluorescent pyrrolinone-type moieties. Decrease in free-lysine residues in HSA exposed to various concentrations of CSE, assessed with the reduction of fluorescamine fluorescence (Fig. 5, inset), occurred progressively with the increasing CSE concentrations, with ∼25% of the fluorescamine fluorescence lost after HSA incubation with 64% CSE (Fig. 5).

Determination of free arginine side chains by using 9,10-phenanthrenequinone revealed that Arg residues were not modified by CSE exposure, at any of the CSE concentrations used (not shown).

Table 2 reports the covalent adducts identified in HSA exposed to different doses of CSE. Several Michael adducts of both α,β-unsaturated aldehydes, acrolein and crotonaldehyde, were identified, involving Cys, His, and Lys residues. In particular, according to our previous studies (3), Cys34 was found to be a reactive nucleophilic site, able to form Michael adducts with both the α,β-unsaturated aldehydes. Structure elucidation of the modified peptides, as well as the adduction sites, was fully characterized by MS/MS analysis. The Fig. 6 exemplary shows the LC-ESI-MS/MS spectra of the HSA tryptic fragment containing the Cys34 residue (ALVLIAFA-QYLQQCPFEDHVK), after HSA incubation in the absence (Fig. 6A) and presence (Fig. 6B) of 16% CSE. The y and b fragmentation pattern well demonstrates the disulfide bond of Cys34 –SH group with the reducing agent β-mercaptoethanol in control HSA (Fig. 6A) and the Michael adduction of acrolein on the Cys34 thiol when HSA was incubated in the presence of 16% CSE (Fig. 6B). We previously found that, besides Cys34, Lys525 is also a reactive nuclophilic target of α,β-unsaturated aldehydes (3). Accordingly, in the present study, we found that Lys525 is covalently adducted through a Michael adduction mechanism by both acrolein and crotonaldehyde. The LC-ESI-MS/MS spectra and the y and b ion fragment attribution of Lys525-containing peptide (KQTAL-VELVK) are shown in Fig. 7 for both control HSA (Fig. 7A) and HSA incubated with 16% CSE (Fig. 7B). His39 also was found to be covalently modified through acrolein and crotonaldehyde Michael adducts (Table 2). Other Michael adducts were identified only at the highest CSE dose, involving Lys351, Lys137 (as acrolein and crotonaldehyde Michael adducts), and His338 (as acrolein Michael adduct). Finally, Lys541 and Lys545 were found to form a Schiff base with acrolein at all the CSE concentration tested, whereas no Schiff base due to reaction with crotonaldehyde was observed (Table 2).

TABLE 2. ACROLEIN- AND CROTONALDEHYDE-MODIFIED HSA PEPTIDES DETECTED BY LC-ESI-MS/MS

Acrolein Michael adduct		
Cysteine	*Lysine*	*Histidine*
ALVLIAFAQYLQQC*PFEDHVK (Cys34)	K*QTALVELVK (Lys525) LAK*TYETTLEK (Lys351)[†] K*YLYEIAR (Lys137)[†]	ALVLIAFAQYLQQCPFEDH*VK (His39) RH*PDYSVVLLLR (His338)[†]
Crotonaldehyde Michael adduct		
ALVLIAFAQYLQQC*PFEDHVK (Cys34)	K*QTALVELVK (Lys525) LAK*TYETTLEK (Lys351)[†] K*YLYEIAR (Lys137)[†]	ALVLIAFAQYLQQCPFEDH*VK (His39)
Acrolein Lysine Schiff base		
	ATK*EQLKAVMDDFAAFVEK (Lys541) ATKEQLK*AVMDDFAAFVEK (Lys545)	

*Adduction site; [†]detected only in 64% CSE-treated samples.
None of the listed covalent modifications were detected in control mercaptalbumin (HSA-SH).

The dose-dependent effect of CSE-induced modifications of Cys34-containing peptide by acrolein and crotonaldehyde Michael adducts is shown in Fig. 8A. An almost linear increase for both the modified peptides is evident up to 16% CSE, whereas a marked reduction of the covalent peptides was observed at a dose of 64% CSE. This reduction might be due to the formation of cross-links involving Cys34 and taking place because of the massive carbonylation of the protein. Figure 8B shows the CSE dose-dependent increase in acrolein adducted to Lys525, which linearly increased up to 64% CSE.

One of the most-applied techniques for determination of protein carbonyl content is the reaction of carbonyl groups with DNPH to form a protein-bound 2,4-dinitrophenylhydrazone, which can be detected spectrophotometrically by its absorbance at 370 nm. The spectrophotometric method developed by Levine and colleagues (31, 32) has become a standard method for quantitative determination of protein carbonylation. The DNPH-derivatized proteins can also be detected immunochemically after SDS-PAGE separation and Western blotting by using anti-DNP antibodies (20). The extent of carbonyl-group formation in HSA exposed to CSE, quantified by using the spectrophotometric DNPH assay, is shown in Fig. 9. Exposure of HSA to 1% and 4% CSE increased only by a small extent the albumin carbonyl content, whereas exposure of HSA to 16% and 64% CSE induced a marked albumin carbonylation (Fig. 9). The results of carbonylation-specific immunochemical detection after SDS-PAGE separation and Western blotting by using anti-DNP antibodies are presented in Fig. 10A: the albumin exposed to CSE clearly exhibited a progressive increase in carbonyl content with the increase in CSE concentration. Comparison of the chemiluminescence image (Fig. 10A) with the CBB-staining image (Fig. 10B) of the same gel demonstrated equal albumin loading in each lane. Densitometric analysis of the chemiluminescence film quantified the relative increase in carbonylation of CSE-treated HSA compared with that of control HSA (mercaptalbumin) (Fig. 10C).

The possibility of preventing CSE-induced HSA carbonylation was investigated by incubating HSA with increasing concentrations of the carbonyl-scavenging drugs hydralazine or pyridoxamine, before exposing the protein to CSE. Carbonyl-scavenging drugs containing thiol or amine functional groups act therapeutically in preventing protein carbonylation by trapping the carbonyl precursors and aldehydes formed during the lipid and sugar oxidation process to form nontoxic adducts. Hydralazine is a vasodilating antihypertensive drug that traps acrolein bound to protein, with formation of the corresponding hydrazone derivatives, and thus reduces the carbonyl stress *in vivo* and prevents acrolein-induced cell toxicity (11, 24). It also is an efficient scavenger of free α,β-unsaturated aldehydes (24). Pyridoxamine is one of the three natural forms of vitamin B_6 and an intermediate in transamination reactions catalyzed by vitamin B_6–dependent enzymes. Pyridoxamine is a potent inhibitor of the chemical modification of proteins (mainly Lys residues) by peroxidizing lipids during lipid-peroxidation (lipoxidation) reactions and traps reactive intermediates formed during lipid peroxidation (42). Pyridoxamine also is an inhibitor of advanced glycoxidation end products (AGEs), and its trapping ability was recently extended to 1,4-dicarbonyls, a class of reactive compounds such as 2,5-hexanedione and endogenous 4-ketoaldehydes (1).

Both hydralazine (a reactive carbonyl species scavenger) (Fig. 11A) and pyridoxamine (a ROS and reactive carbonyl species scavenger) (Fig. 11B) significantly prevented CSE-induced HSA carbonylation at the higher concentration tested (1 m*M*), the latter also being efficient in preventing carbonylation at micromolar concentrations (Fig. 11).
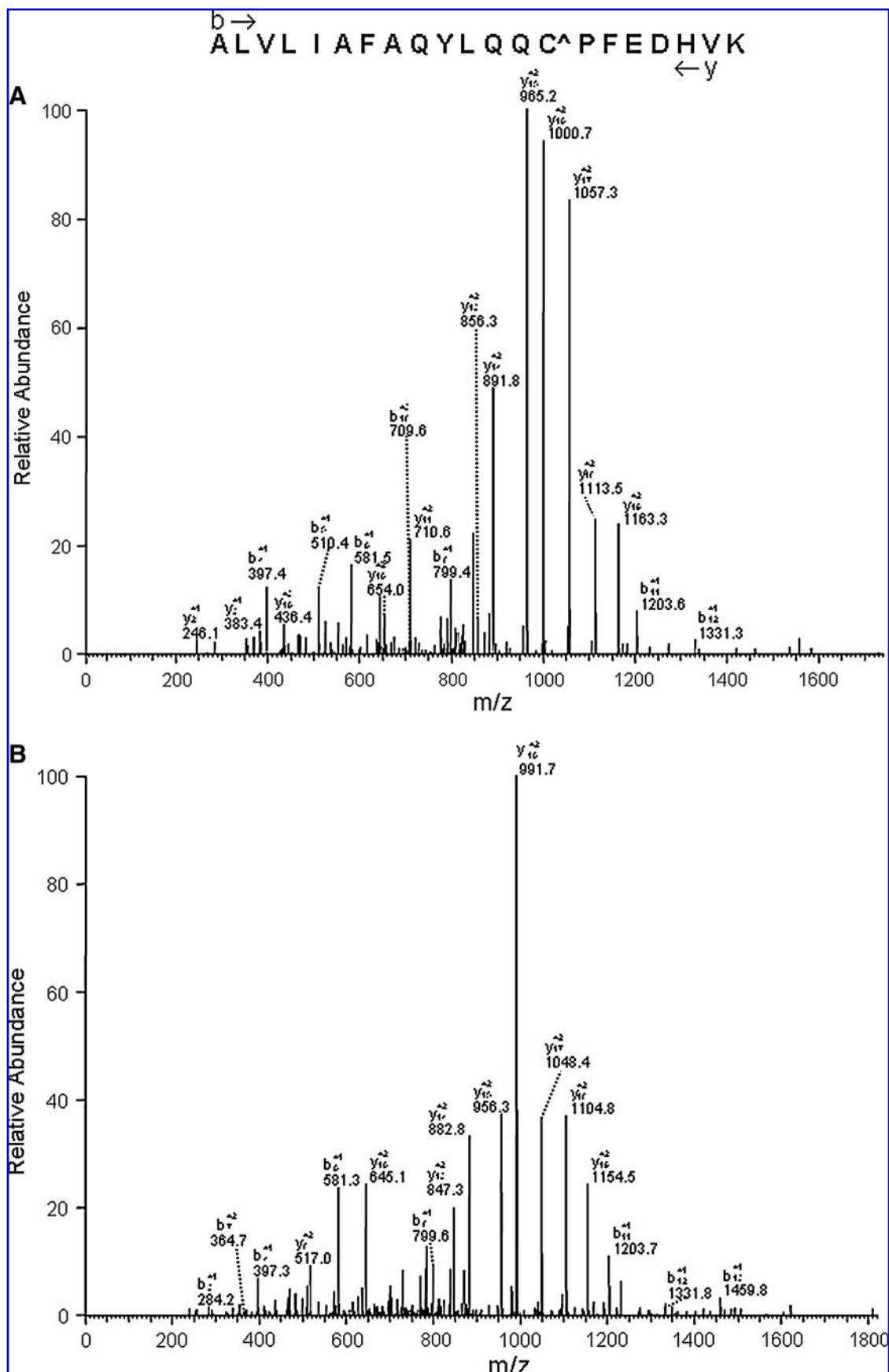
FIG. 6. **LC-ESI-MS/MS spectra of HSA tryptic fragment ALVLIAFAQYLQQCPFEDHVK.** (**A**) Control HSA (HSA-SH). The spectrum shows the product ions of the precursor $[M+3H]^{3+}$ at m/z 837.42619. Cys34 is found as disulfide with the reducing agent β-mercaptoethanol. (**B**) HSA incubated with 16% CSE. The spectrum shows the product ions of the precursor $[M+3H]^{3+}$ at m/z 831.44092. Cys34 is modified by an acrolein Michael adduct. Modified fragment ions are labeled with an asterisk according to the nomenclature of peptide fragmentation.

FIG. 7. LC-ESI-MS/MS spectra of HSA tryptic fragment KQTALVELVK. HSA was incubated with 16% CSE, reduced with NaBH$_4$, and then digested by trypsin in reducing conditions. The figure shows the product ions of the peptides covalently adducted by acrolein (**A**, precursor ion [M+2H]$^{2+}$ at m/z 593.87380) and by crotonaldehyde (**B**, precursor ion [M+2H]$^{2+}$ at m/z 600.881719). Lys525 was found to be the adduction site.
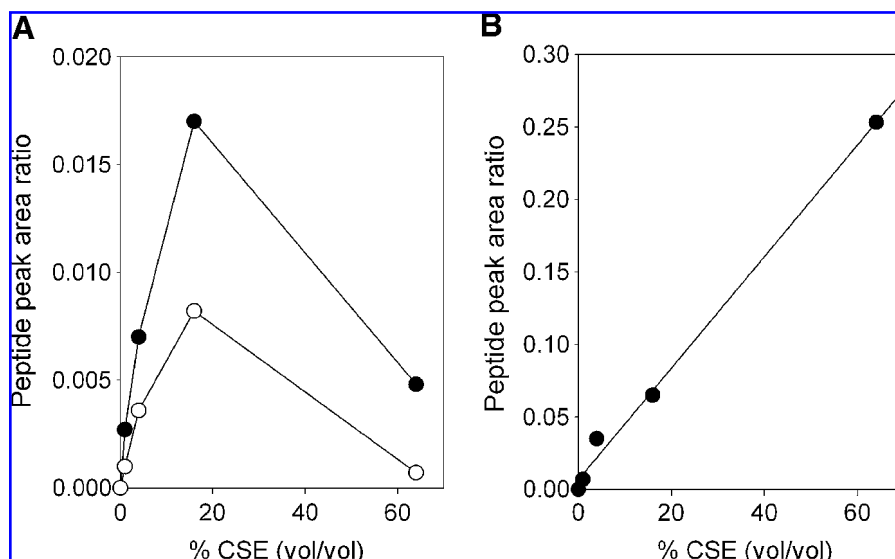
FIG. 8. Acrolein and crotonaldehyde covalent modifications of Cys34- and Lys525-containing peptides. (A) Dose-dependent formation of acrolein (●) and crotonaldehyde (○) Michael adducts of Cys34-containing peptide. (B) Dose-dependent formation of covalently acrolein-modified peptide KQTAL-VELVKACR (K525 was found to be the adduction site). Peptide peak-area ratios were calculated as described in Materials and Methods and by using the LSQR peptide as reference.

Discussion

Albumin accounts for ∼60% of total protein in the plasma of healthy people, being typically present at a concentration of ∼0.6 mM (∼43 mg/ml) (44). Albumin is the main determinant of plasma oncotic pressure and exhibits many other biologic functions, such as transport of endogenous and exogenous compounds (e.g., such as free fatty acids, hormones, and drugs), modulation of capillary permeability, and neutrophil adhesion and activation (38, 44). Interestingly, an important amount of albumin is localized extravascularly (44). Actually, the albumin pool present in extravascular/extracellular compartments represents more than double the intravascular pool. Albumin is the largest (>80%) thiol pool in

FIG. 9. Total carbonyl formation in CSE-treated HSA. HSA-SH solutions were treated with vehicle (control) or 1%, 4%, 16%, and 64% (vol/vol) CSE and exhaustively dialyzed against PBS. Carbonyl formation was assessed with spectrophotometric assay from the absorbance at 366 nm after DNPH derivatization, as described in Materials and Methods. Data are presented as the mean ± SD of three replicate measurements.

plasma owing to its only free cysteine, Cys34. In healthy adults, ∼70% of total HSA contains the free sulfhydryl group of Cys34 (human mercaptalbumin, HSA-SH); ∼25% of the Cys34 forms a mixed disulfide with low-molecular-weight thiols, like another cysteine, homocysteine, cysteinylglycine, or glutathione, generating S-thiolated albumin, the predominant modification being S-cysteinylation (30, 48); a small fraction of the Cys34 is more highly oxidized to the sulfinic or sulfonic acid form (52). Although HSA-SH does not react particularly fast with oxidants, it can still be considered to be an important plasma scavenger and a key element of antioxidant defenses due to its very high concentration (0.4–0.5 mM) (12, 23, 30, 52). A central intermediate in this potential antioxidant activity of HSA is the sulfenic acid form of Cys34 (HSA-SOH) (12, 51, 52). However, it is documented that HSA is quite vulnerable to reactive species (8, 12). Many studies have shown the presence of elevated levels of carbonylated albumin in patients with various diseases (7, 27, 35, 37, 39).

Most of the plasma-protecting activity against oxidative/carbonyl stress has been attributed to the presence of urate and proteins, especially albumin (10). A number of studies have reported significantly elevated levels of plasma protein carbonyls in smokers compared with matched nonsmokers (34, 45). Albumin is the major carbonylated protein in the bronchoalveolar lavage fluid in older smokers (36, 50). Recently, we proposed that HSA, through nucleophilic residues, in particular Cys34, can act as an endogenous detoxifying agent of circulating reactive carbonyl species in human plasma (4). One can then hypothesize that α,β-unsaturated aldehydes can be major mediators of CS-induced albumin carbonylation.

In this study, we identified the exact α,β-unsaturated aldehyde covalent adducts and relative position of the modification in human mercaptalbumin exposed to various concentrations of whole-phase CSE. Potential Cys, His, and Lys residues for the formation of α,β-unsaturated aldehyde covalent adducts, with their relative surface accessibility, and predicted acrolein and crotonaldehyde covalent adducts on HSA are shown in Fig. 1 and Table 1, respectively.

The increase in the 350- to 550-nm emission fluorescence intensity of HSA samples exposed to increasing concentra-
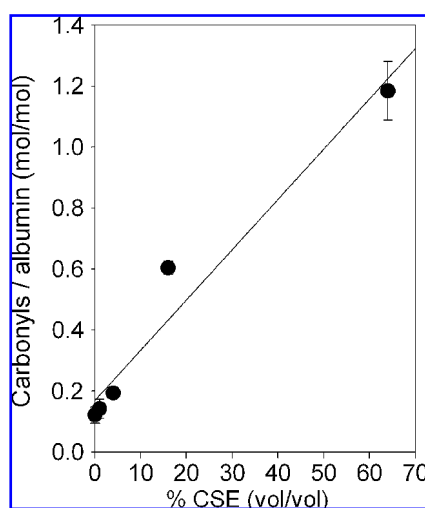
FIG. 10. **Total carbonyl formation in CSE-treated HSA.** HSA-SH solutions were treated with vehicle (control) or 1%, 4%, 16%, and 64% (vol/vol) CSE and exhaustively dialyzed against PBS. (**A**) The increase in HSA carbonyl content was assessed as DNP-protein adducts with Western immunoblotting probed with anti-DNP antibodies and visualized with enhanced chemiluminescence, as described in Materials and Methods. (**B**) The same gel stained with CBB. (**C**) Densitometric analysis of carbonyl content. Changes in carbonylation signal in comparison with carbonylation of control HSA (HSA-SH), considered as 100%, are shown. Data are presented as the mean ± SD of three replicate measurements.
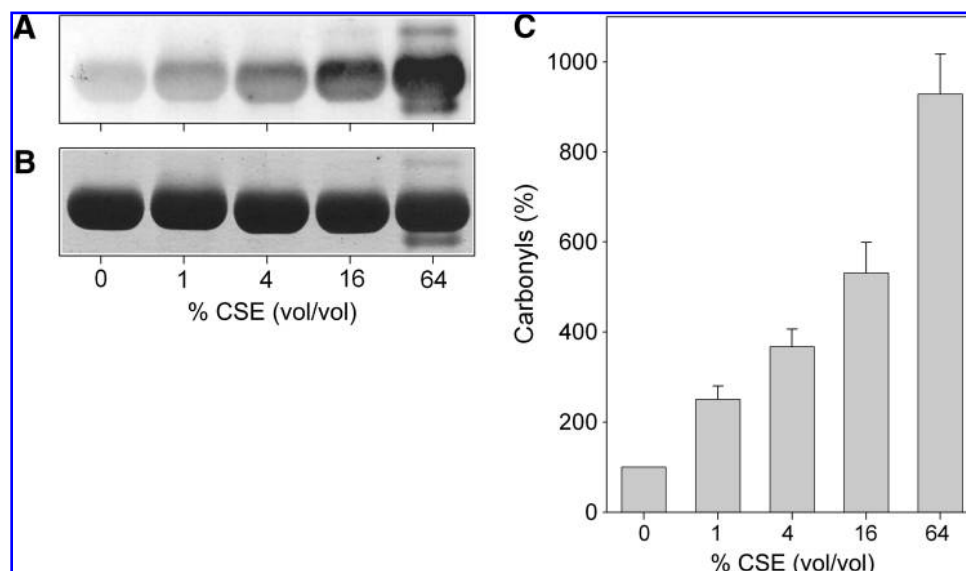
tions of CSE indicates that some water-soluble components of mainstream CS are bound to albumin (Fig. 2).

Exposure of human mercaptalbumin to increasing concentrations of CSE progressively induced a marked decrease in the relative concentration of Cys34 free thiol, whose level (and therefore that of HSA-SH) was only 10% of bulk HSA after exposure to 16% and 64% CSE, as shown by the decreased binding of the sulfhydryl-reactive fluorophore AMCA-HPDP (Figs. 3 and 4), and a loss of the ε-amino group of lysine residues, as shown by the reduction of fluorescamine fluorescence (Fig. 5). Taken together, these results suggest covalent adduction of α,β-unsaturated aldehydes derived from mainstream CS to Cys and Lys residues in HSA exposed to various concentrations of whole-phase CSE. This was

confirmed by LC-ESI-MS/MS analyses (Figs. 6 through 8), which evidenced the formation of both acrolein (at Cys34, His39, Lys137, His338, Lys351, and Lys525) and crotonaldehyde (at Cys34, His39, Lys137, Lys351, and Lys525) Michael adducts. LC-ESI-MS/MS analysis also identified other two adducted peptides, deriving from the formation of a Schiff base adduct of acrolein with Lys541 and Lys545 (Table 2). As expected, α,β-unsaturated aldehydes covalent adduction resulted in a marked increase in HSA carbonylation, as measured by both spectrophotometric determination and Western immunoblotting with anti-DNP antibodies after DNPH-derivatization of protein carbonyls (Figs. 9 and 10).

Finally, the carbonyl-scavenger drugs, hydralazine and pyridoxamine, partially prevented CSE-induced HSA

FIG. 11. **Effect of carbonyl scavenger activity on CSE-induced HSA carbonylation.** HSA-SH solutions were incubated with vehicle (control; ●) or 10 μM (◇), 100 μM (□), or 1 mM (○) hydralazine (**A**) or pyridoxamine (**B**), for 60 min, before exposing protein solutions to 1%, 4%, 16%, and 64% (vol/vol) CSE, for 60 min. After protein precipitation with 20% (final concentration) TCA, protein carbonylation was quantified with the spectrophotometric assay with DNPH, as described in Materials and Methods. Data are presented as the mean ± SD of three replicate measurements.
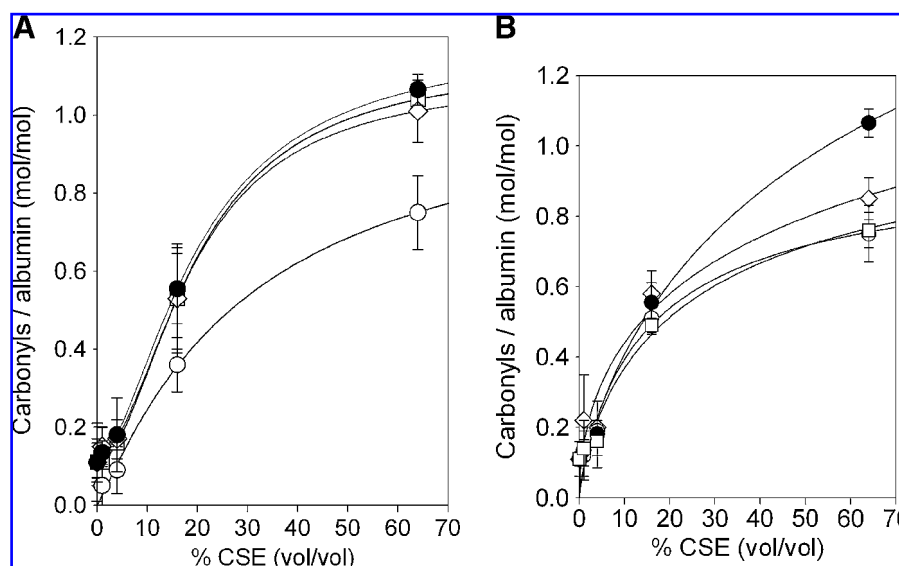
carbonylation, the latter being more effective also at micromolar concentrations (Fig. 11).

As a whole, our observations raise the possibility that albumin carbonylation induced by tobacco smoke (36, 50) can be, at least in part, attributable to water-soluble α,β-unsaturated aldehydes of CS. We cannot exclude that other oxidative modifications contributed to albumin carbonylation, but our observations suggest that α,β-unsaturated aldehyde–induced carbonylation of Cys, Lys, and His residues is preponderant.

α,β-Unsaturated aldehyde adducts on albumin can be of particular interest to smokers, because the use of albumin as biomarker of oxidative/carbonyl stress can be more useful than others for larger studies, given that HSA is present in higher concentrations in blood than is DNA or other proteins, is not subject to enzymatic repair, carbonylated albumin is relatively stable, and only small amounts of plasma are required for analysis. A key question when considering the significance of albumin carbonylation associated with CS is whether this can be simply a biomarker for the presence of oxidative/carbonyl stress or this can have some substantive consequence on physiologic HSA functions. Other several questions must be addressed, such as (a) does covalent HSA adduction by α,β-unsaturated aldehydes impair its functional properties? For instance, its antioxidant properties, its binding of plasma low-molecular-weight thiols or its buffer function for nitric oxide through S-nitrosylation of Cys34 (38), the latter resulting in a detrimental release of nitric oxide? (b) Does covalent HSA adduction by α,β-unsaturated aldehydes change the ligand-binding properties of drugs with important therapeutic role in human diseases? (c) May α,β-unsaturated aldehydes become new pharmacologic targets for carbonyl-sequestering agents in smokers? In principle, most (if not each) modifications of the protein can be expected to modify its conformation and hence its binding properties.

The introduction of carbonyl derivatives can modify the conformation of the polypeptide chain, thus determining the partial or total inactivation of proteins (17–19). Carbonylation of HSA associated with cigarette smoking may result in modifications of its biologic properties. Depletion of Cys34 free sulfhydryl group could potentially results in a marked decrease in circulating antioxidant thiols in smokers, as HSA comprises the largest thiol pool in plasma. It is plausible that perturbations in plasma thiol redox could be a contributory mechanism to the promotion of multiorgan chronic disease by smoking. A disturbed transport function of carbonylated serum albumin can impair intercellular and interorgan traffic of endogenous compounds such as fatty acids, bilirubin, and hormones, as well as delivery of a long list of exogenous compounds (*e.g.*, antibiotics). Thus, albumin also affects the pharmacokinetics of several drugs. For instance, the single Cys34 thiol in albumin is capable of reacting with a wide variety of biologically important molecules and forms disulfides with the drugs disulfiram (a drug used for ∼50 years in the treatment of alcoholism, whose anticancer activity has recently been disclosed), captopril (a thiol-containing angiotensin converting enzyme inhibitor), with anticancer thiol-binding doxorubicin derivatives or with gold(I) from antiarthritic drugs like auranofin (38). Cys34 thiol can also be modified by other drugs like the diuretic ethacrynic acid or penicillin. Whereas Lys525 is located within the diazepam binding site and is also the preferred binding of homocysteine (38).

This study also suggests that the development of therapeutic approaches to control α,β-unsaturated aldehyde-induced carbonylation of HSA, which could be involved in some of the pathophysiological conditions associated with oxidative/carbonyl stress induced by CS, might be potentially beneficial in preventing, or attenuating, smoke-related pathological conditions characterized by oxidative/carbonyl stress. Acrolein and other α,β-unsaturated aldehydes could therefore be potential pharmacologic targets for intervention strategies with carbonyl-sequestering agent in smokers in order to inhibit reactive carbonyl species-induced protein carbonylation and hence to improve plasma mercaptalbumin homeostasis (1).

Acknowledgments

Author Disclosure Statement

No competing financial interests exist.

References

1. Aldini G, Dalle-Donne I, Facino RM, Milzani A, and Carini M. Intervention strategies to inhibit protein carbonylation by lipoxidation-derived reactive carbonyls. *Med Res Rev* 27: 817–868, 2007.
2. Aldini G, Dalle-Donne I, Vistoli G, Maffei Facino R, and Carini M. Covalent modification of actin by 4-hydroxy-trans-2-nonenal (HNE): LC-ESI-MS/MS: evidence for Cys374 Michael adduction. *J Mass Spectrom* 40: 946–954, 2005.
3. Aldini G, Gamberoni L, Orioli M, Beretta G, Regazzoni L, Maffei Facino R, and Carini M. Mass spectrometric characterization of covalent modification of human serum albumin by 4-hydroxy-trans-2-nonenal. *J Mass Spectrom* 41: 1149–1161, 2006.
4. Aldini G, Vistoli G, Regazzoni L, Gamberoni L, Facino RM, Yamaguchi S, Uchida K, and Carini M. Albumin is the main nucleophilic target of human plasma: a protective role against pro-atherogenic electrophilic reactive carbonyl species? *Chem Res Toxicol* 21: 824–835, 2008.
5. Andreoli R, Manini P, Corradi M, Mutti A, and Niessen WM. Determination of patterns of biologically relevant aldehydes in exhaled breath condensate of healthy subjects by liquid chromatography/atmospheric chemical ionization tandem mass spectrometry. *Rapid Commun Mass Spectrom* 17: 637–645, 2003.
6. Annovazzi L, Cattaneo V, Viglio S, Perani E, Zanone C, Rota C, Pecora F, Cetta G, Silvestri M, and Iadarola P. High-performance liquid chromatography and capillary electrophoresis: methodological challenges for the determination of biologically relevant low-aliphatic aldehydes in human saliva. *Electrophoresis* 25: 1255–1263, 2004.
7. Anraku M, Kitamura K, Shinohara A, Adachi M, Suenga A, Maruyama T, Miyanaka K, Miyoshi T, Shiraishi N, Nonoguchi H, Otagiri M, and Tomita K. Intravenous iron administration induces oxidation of serum albumin in

hemodialysis patients. *Kidney Int* 66: 841–848, 2004. Erratum in: *Kidney Int* 66: 1304, 2004.

8. Anraku M, Yamasaki K, Maruyama T, Kragh-Hansen U, and Otagiri M. Effect of oxidative stress on the structure and function of human serum albumin. *Pharm Res* 18: 632–639, 2001.

9. Bartecchi CE, Mackenzie TD, and Schier RW. The human costs of tobacco use. *N Engl J Med* 330: 907–912, 1994.

10. Bourdon E and Blache D. The importance of proteins in defense against oxidation. *Antioxid Redox Signal* 3: 293–311, 2001.

11. Burcham PC and Pyke SM. Hydralazine inhibits rapid acrolein-induced protein oligomerization: role of aldehyde scavenging and adduct trapping in cross-link blocking and cytoprotection. *Mol Pharmacol* 69: 1056–1065, 2006.

12. Carballal S, Radi R, Kirk MC, Barnes S, Freeman BA, and Alvarez B. Sulfenic acid formation in human serum albumin by hydrogen peroxide and peroxynitrite. *Biochemistry* 42: 9906–9914, 2003.

13. Carmella SG, Chen M, Zhang Y, Zhang S, Hatsukami DK, and Hecht SS. Quantitation of acrolein-derived (3-hydroxypropyl)mercapturic acid in human urine by liquid chromatography-atmospheric pressure chemical ionization tandem mass spectrometry: effects of cigarette smoking. *Chem Res Toxicol* 20: 986–990, 2007.

14. Clunes LA, Bridges A, Alexis N, and Tarran R. In vivo versus in vitro airway surface liquid nicotine levels following cigarette smoke exposure. *J Anal Toxicol* 32: 201–207, 2008.

15. Conklin DJ, Haberzettl P, Prough RA, and Bhatnagar A. Glutathione S-transferase P protects against endothelial dysfunction induced by exposure to tobacco smoke. *Am J Physiol Heart Circ Physiol* 2009, doi:10.1152/ajpheart.00867.2008.

16. Csiszar A, Labinskyy N, Podlutsky A, Kaminski PM, Wolin MS, Zhang C, Mukhopadhyay P, Pacher P, Hu F, de Cabo R, Ballabh P, and Ungvari Z. Vasoprotective effects of resveratrol and SIRT1: attenuation of cigarette smoke-induced oxidative stress and proinflammatory phenotypic alterations. *Am J Physiol Heart Circ Physiol* 294: H2721–H2735, 2008.

17. Dalle-Donne I, Aldini G, Carini M, Colombo R, Rossi R, and Milzani A. Protein carbonylation, cellular dysfunction, and disease progression. *J Cell Mol Med* 10: 389–406, 2006.

18. Dalle-Donne I, Carini M, Vistoli G, Gamberoni L, Giustarini D, Colombo R, Maffei Facino R, Rossi R, Milzani A, and Aldini G. Actin Cys374 as a nucleophilic target of alpha, beta-unsaturated aldehydes. *Free Radic Biol Med* 42: 583–598, 2007.

19. Dalle-Donne I, Rossi R, Gagliano N, Milzani A, Di Simplicio P, and Colombo R. Actin carbonylation: from simple marker of protein oxidation to relevant sign of severe functional impairment. *Free Radic Biol Med* 31: 1075–1083, 2001.

20. Dalle-Donne I, Rossi R, Giustarini D, Milzani A, and Colombo R. Protein carbonyl groups as biomarkers of oxidative stress. *Clin Chim Acta* 329: 23–38, 2003.

21. Eckenhoff RG, Petersen CE, Ha CE, and Bhagavan NV. Inhaled anesthetic binding sites in human serum albumin. *J Biol Chem* 275: 30439–30444, 2000.

22. Esterbauer H, Schaur RJ, and Zollner H. Chemistry and biochemistry of 4-hydroxynonenal, malonaldehyde, and related aldehydes. *Free Radic Biol Med* 11: 81–128, 1991.

23. Faure P, Troncy L, Lecomte M, Wiernsperger N, Lagarde M, Ruggiero D, and Halimi S. Albumin antioxidant capacity is modified by methylglyoxal. *Diabetes Metab* 31: 169–177, 2005.

24. Galvani S, Coatrieux C, Elbaz M, Grazide MH, Thiers JC, Parini A, Uchida K, Kamar N, Rostaing L, Baltas M, Salvayre R, and Nègre-Salvayre A. Carbonyl scavenger and anti-atherogenic effects of hydrazine derivatives. *Free Radic Biol Med* 45: 1457–1467, 2008.

25. Guex N and Peitsch MC. SWISS-MODEL and the Swiss-Pdbviewer: an environment for comparative protein modeling. *Electrophoresis* 18: 2714–2723, 1997.

26. Han P, Zhou X, Huang B, Zhang X, and Chen C. On-gel fluorescent visualization and the site identification of S-nitrosylated proteins. *Anal Biochem* 377: 150–155, 2008.

27. Himmelfarb J and McMonagle E. Albumin is the major plasma protein target of oxidant stress in uremia. *Kidney Int* 60: 358–363, 2001.

28. Hoffmann D, Hoffmann I, and El-Bayoumy K. The less harmful cigarette: a controversial issue: a tribute to Ernst L. Wynder. *Chem Res Toxicol* 14: 767–790, 2001.

29. Ishii T, Matsuse T, Igarashi H, Masuda M, Teramoto S, and Ouchi Y. Tobacco smoke reduces viability in human lung fibroblasts: protective effect of glutathione S-transferase P1. *Am J Physiol Lung Cell Mol Physiol* 280: L1189–L1195, 2001.

30. Kawakami A, Kubota K, Yamada N, Tagami U, Takehana K, Sonaka I, Suzuki E, and Hirayama K. Identification and characterization of oxidized human serum albumin: a slight structural change impairs its ligand-binding and antioxidant functions. *FEBS J* 273: 3346–3357, 2006.

31. Levine RL, Wehr N, Williams JA, Stadtman ER, and Shacter E. Determination of carbonyl groups in oxidized proteins. *Methods Mol Biol* 99: 15–24, 2000.

32. Levine RL, Williams JA, Stadtman ER, and Shacter E. Carbonyl assays for determination of oxidatively modified proteins. *Methods Enzymol* 233: 346–357, 1994.

33. Lu X, Cai J, Kong H, Wu M, Hua R, Zhao M, Liu J, and Xu G. Analysis of cigarette smoke condensates by comprehensive two-dimensional gas chromatography/time-of-flight mass spectrometry I acidic fraction. *Anal Chem* 75: 4441–4451, 2003.

34. Marangon K, Devaraj S, and Jialal I. Measurement of protein carbonyls in plasma of smokers and in oxidized LDL by an ELISA. *Clin Chem* 45: 577–578, 1999.

35. Mera K, Anraku M, Kitamura K, Nakajou K, Maruyama T, Tomita K, and Otagiri M. Oxidation and carboxy methyl lysine-modification of albumin: possible involvement in the progression of oxidative stress in hemodialysis patients. *Hypertens Res* 28: 973–980, 2005.

36. Nagai K, Betsuyaku T, Kondo T, Nasuhara Y, and Nishimura M. Long term smoking with age builds up excessive oxidative stress in bronchoalveolar lavage fluid. *Thorax* 61: 496–502, 2006.

37. Nagai K, Betsuyaku T, Konno S, Ito Y, Nasuhara Y, Hizawa N, Kondo T, and Nishimura M. Diversity of protein carbonylation in allergic airway inflammation. *Free Radic Res* 42: 921–929, 2008.

38. Oettl K and Stauber RE. Physiological and pathological changes in the redox state of human serum albumin critically influence its binding properties. *Br J Pharmacol* 151: 580–590, 2007.

39. Oettl K, Stadlbauer V, Petter F, Greilberger J, Putz-Bankuti C, Hallström S, Lackner C, and Stauber RE. Oxidative damage of albumin in advanced liver disease. *Biochim Biophys Acta* 1782: 469–473, 2008.

40. Olsen JV, de Godoy LM, Li G, Macek B, Mortensen P, Pesch R, Makarov A, Lange O, Horning S, and Mann M. Parts per million mass accuracy on an Orbitrap mass spectrometer via lock mass injection into a C-trap. *Mol Cell Proteomics* 4: 2010–2021, 2005.

41. O'Neill CA, Halliwell B, van der Vliet A, Davis PA, Packer L, Tritschler H, Strohman WJ, Rieland T, Cross CE, and Reznick AZ. Aldehyde-induced protein modifications in human plasma: protection by glutathione and dihydrolipoic acid. *J Lab Clin Med* 124: 359–370, 1994.

42. Onorato JM, Jenkins AJ, Thorpe SR, and Baynes JW. Pyridoxamine, an inhibitor of advanced glycation reactions, also inhibits advanced lipoxidation reactions: mechanism of action of pyridoxamine. *J Biol Chem* 275: 21177–21184, 2000.

43. Panda K, Chattopadhyay R, Ghosh MK, Chattopadhyay DJ, and Chatterjee IB. Vitamin C prevents cigarette smoke induced oxidative damage of proteins and increased proteolysis *Free Radic Biol Med* 27: 1064–1079, 1999.

44. Peters T Jr. The albumin molecule: structure and chemical properties. In: *All about Albumin: Biochemistry, Genetics, and Medical Applications*, edited by Peters T Jr. San Diego, CA: Academic Press, 1996, pp. 9–75.

45. Pignatelli B, Li CQ, Boffetta P, Chen Q, Ahrens W, Nyberg F, Mukeria A, Bruske-Hohlfeld I, Fortes C, Constantinescu V, Ischiropoulos H, and Ohshima H. Nitrated and oxidized plasma proteins in smokers and lung cancer patients. *Cancer Res* 61: 778–784, 2001.

46. Pryor WA and Stone K. Oxidants in cigarette smoke: radicals, hydrogen peroxides, peroxynitrate and peroxynitrite. *Ann N Y Acad Sci* 686: 12–28, 1993.

47. Reznick AZ, Cross CE, Hu ML, Suzuki YJ, Khwaja S, Safadi A, Motchnik PA, Packer L, and Halliwell B. Modification of plasma proteins by cigarette smoke as measured by protein carbonyl formation. *Biochem J* 286: 607–611, 1992.

48. Rossi R, Giustarini D, Milzani A, and Dalle-Donne I. Cysteinylation and homocysteinylation of plasma protein thiols during ageing of healthy human beings. *J Cell Mol Med* 2008, doi:10.1111/j.1582–4934.2008.00417.x.

49. Schmitt A, Schmitt J, Münch G, and Gasic-Milencovic J. Characterization of advanced glycation end products for biochemical studies: side chain modifications and fluorescence characteristics. *Anal Biochem* 338: 201–215, 2005.

50. Suzuki M, Betsuyaku T, Ito Y, Nagai K, Nasuhara Y, Kaga K, Kondo S, and Nishimura M. Down-regulated NF-E2–related factor 2 in pulmonary macrophages of aged smokers and patients with chronic obstructive pulmonary disease. *Am J Respir Cell Mol Biol* 39: 673–682, 2008.

51. Turell L, Botti H, Carballal S, Ferrer-Sueta G, Souza JM, Durán R, Freeman BA, Radi R, and Alvarez B. Reactivity of sulfenic acid in human serum albumin. *Biochemistry* 47: 358–367, 2008.

52. Turell L, Botti H, Carballal S, Radi R, and Alvarez B. Sulfenic acid: a key intermediate in albumin thiol oxidation. *J Chromatogr B Analyt Technol Biomed Life Sci* 877: 3384–3392, 2008.

53. Weiner D, Levy Y, Khankin EV, and Reznick AZ. Inhibition of salivary amylase activity by cigarette smoke aldehydes. *J Physiol Pharmacol* 59: 727–737, 2008.

Address correspondence to:
Isabella Dalle-Donne, Ph.D.
Department of Biology
University of Milan
via Celoria 26
I-20133 Milan, Italy

E-mail: quack@unimi.it

Abbreviations Used

AMCA-HPDP = *N*-[6,7-(amino-4-methylcoumarin-3-acetamido)hexyl]-3'-[2'-pyridyldithio] propionamide
CBB = Coomassie brilliant blue
CS = cigarette smoke
CSE = cigarette smoke extract
DNP = dinitrophenyl
DNPH = dinitrophenyl hydrazine
HSA = human serum albumin
MS = mass spectrometry
nanoLC-ESI-MS/MS = nanoscale liquid chromatography electrospray ionization tandem mass spectrometry
RNS = reactive nitrogen species
ROS = reactive oxygen species
SDS-PAGE = sodium dodecylsulfate-polyacrylamide gel electrophoresis
TCA = trichloroacetic acid

This article has been cited by:

1. Graziano Colombo , Marco Clerici , Daniela Giustarini , Ranieri Rossi , Aldo Milzani , Isabella Dalle-Donne . 2012. Redox Albuminomics: Oxidized Albumin in Human Diseases. *Antioxidants & Redox Signaling* **17**:11, 1515-1527. [Abstract] [Full Text HTML] [Full Text PDF] [Full Text PDF with Links] [Supplemental material]

2. Albumin **5**, 83-182. [CrossRef]

3. Oren Rom, Sharon Kaisari, Dror Aizenbud, Abraham Z. Reznick. 2012. Identification of possible cigarette smoke constituents responsible for muscle catabolism. *Journal of Muscle Research and Cell Motility* **33**:3-4, 199-208. [CrossRef]

4. Zafer Ugur, Chelsea M. Coffey, Scott Gronert. 2012. Comparing the efficiencies of hydrazide labels in the study of protein carbonylation in human serum albumin. *Analytical and Bioanalytical Chemistry* . [CrossRef]

5. Gabriella Fanali, Alessandra di Masi, Viviana Trezza, Maria Marino, Mauro Fasano, Paolo Ascenzi. 2012. Human serum albumin: From bench to bedside. *Molecular Aspects of Medicine* **33**:3, 209-290. [CrossRef]

6. Alice Gualerzi, Michele Sciarabba, Gianluca Tartaglia, Chiarella Sforza, Elena Donetti. 2012. Acute effects of cigarette smoke on three-dimensional cultures of normal human oral mucosa. *Inhalation Toxicology* **24**:6, 382-389. [CrossRef]

7. Graziano Colombo, Isabella Dalle-Donne, Marica Orioli, Daniela Giustarini, Ranieri Rossi, Marco Clerici, Luca Regazzoni, Giancarlo Aldini, Aldo Milzani, D. Allan Butterfield, Nicoletta Gagliano. 2012. Oxidative damage in human gingival fibroblasts exposed to cigarette smoke. *Free Radical Biology and Medicine* **52**:9, 1584-1596. [CrossRef]

8. Qingyuan Liu, David C. Simpson, Scott Gronert. 2012. The reactivity of human serum albumin toward trans-4-hydroxy-2-nonenal. *Journal of Mass Spectrometry* **47**:4, 411-424. [CrossRef]

9. Arunava Ghosh, Aparajita Choudhury, Archita Das, Nabendu S. Chatterjee, Tanusree Das, Rukhsana Chowdhury, Koustubh Panda, Rajat Banerjee, Indu B. Chatterjee. 2011. Cigarette smoke induces p-benzoquinone–albumin adduct in blood serum: Implications on structure and ligand binding properties. *Toxicology* . [CrossRef]

10. Giancarlo Aldini, Marica Orioli, Marina Carini. 2011. Protein modification by acrolein: Relevance to pathological conditions and inhibition by aldehyde sequestering agents. *Molecular Nutrition & Food Research* n/a-n/a. [CrossRef]

11. Giancarlo Aldini, Kyung-Jin Yeum, Giulio VistoliCovalent Modifications of Albumin Cys34 as a Biomarker of Mild Oxidative Stress 229-241. [CrossRef]

12. Yuichiro J. Suzuki , Marina Carini , D. Allan Butterfield . 2010. Protein Carbonylation. *Antioxidants & Redox Signaling* **12**:3, 323-325. [Citation] [Full Text HTML] [Full Text PDF] [Full Text PDF with Links]